REAL-TIME CONTROL FOR A MAGNETORHEOLOGICAL SHOCK ABSORBER IN A DRIVER SEAT

BOGDAN SAPIŃSKI

Department of Process Control, University of Science and Technology, Cracow
e-mail: deep@agh.edu.pl

The paper summarizes the author's research study on real-time control of a magnetorheological shock absorber (MRA) in a driver seat. The performance of the MRA for vibration and shock isolation of the driver seat was investigated experimentally in open loop and feedback system configurations. Real-time controllers for MRAs with *on-off* and continuously variable control schemes were developed in the integrated design and control environment of MATLAB/Simulink. The sensors used in experiments were tested to see how reconstructed velocity signals should affect output signals of the controllers to the MRA.

Key words: magnetorheological shock absorber, driver seat, vibrations, shocks, sensor, real-time controller

1. Introduction

Professional drivers spend a great deal of time behind the wheel where they are exposed to vibrations and shocks when their vehicles encounter irregularities of road conditions. The undesired inputs are transmitted to the driver by vehicle sub-systems, when the seat suspension runs out of travel. The truck drivers call that phenomenon "topping" and "bottoming". The topping can injure a driver while the bottoming can lead to loss of control of a vehicle. The risk of the occurrence of that phenomena increases particularly for drivers who adjust the seat height away from the center of the travel. To measure the vibration exposure, the International Standard Organization (ISO) recommends a method called the Vibration Dose Value (VDV). In accordance with that method, the vibration exposure involves numerous shock events.

It is well known that the human body is most sensitive to seat vibrations in the range of $(4,8)$ Hz, so the seats are designed to effectively isolate the

driver from vibrations in this range. In on-highway trucks, most suspensions of conventional driver seats are passive as they employ an air-ride suspension and a passive damper to vibro-isolate the driver. Those seat suspension designs always sacrifice certain degree of either vibration or shock isolation. Such seats are too soft to prevent the driver from the topping and bottoming, and even elastomer snubbers or stiffened springs and/or dampers in seat designs do not provide adequate protection for the driver. For this reason, some driver seats are equipped with semi-active or active suspensions. That allows the drivers to feel more comfortable and less fatigued, and besides gives them better protection.

A smart semi-active solution for the driver seat suspensions is called the Motion Master® Ride Management System (MMS) (http://www.lord.com). The MMS is intended for seat suspensions in trucks, buses and tractors and is used in pupil transportation, trucking and transient industries. Main features of the MMS are: the smoothest air ride without topping and bottoming, automatic vibration and shock control (500 times/sec), prevention end-stop collisions – regardless of driver weight. Results of experiments using a prototype of the MMS revealed that the overall performance of the vibration dose decreased by up to 40%, depending of the seat height.

The MMS includes three components: an MRA containing Lord Corporation's patented Rheontic^{TM} MR fluid, controller that continuously monitors seat motion and determines the optimal damping force, ride mode switch, allowing one to choose among soft, medium or firm settings, following the driver's preference. The system is powered directly from the common 12-volt automotive source. The force produced by the MRA in the MMS is controlled by the use of a controller which adjusts the current driver connected to the MRA coil to the current operating conditions. The controller can be programmed in accordance with an assumed control scheme.

Control methods in semi-active suspensions are classified into *on-off* and continuous categories (Ahmadian, 1999). The methods made use of velocity signals from suspension components. The category of *on-off* methods involves the switching of the suspension system from the minimal (*on*) to maximal (*off*) positions which correspond to the minimal and maximal damping states for the MRA. One of these methods was patented for an MRA used in seat supports (U.S. Patent 5,712, 783, 1998). This is a modified-skyhook method that enables simple, inexpensive hardware to be used and actually outperforms skyhook theoretical control. In order to avoid the harsh feel of end stop collision, end stop limits are suggested to be used to increase the damping force when the damper is about the bottom or top position. Continuous control

methods allows us to enhance the number of switching levels of damping for the suspension as a continuously variable damping coefficient may be achieved (Sapiński, 2005).

In this study, we present examination of the problem how the MRA could protect the driver from vibrations and shocks in a system with the open loop configuration (for constant levels of current applied to the MRA coil) and with the feedback configuration (current levels adjusted by real-time controllers). The real-time operation means here an ability of an MRA control system to follow up the changes in damping of vibration and shock. The experiments were run in a laboratory setup equipped with an adopted driver seat equipped with a commercial MRA of RD-1005-3 series (http://www.lord.com), a current driver engineered for the purpose of the author's research program and data acquisition and control system based on a PC with a multipurpose I/O board, operating in MS-Windows through the MATLAB/Simulink environment. For the purpose of measurement, we used two transformer linear displacement transmitters. Experiments for the driver seat were proceeded by testing the sensors that could be used in the measurement system of the laboratory setup for the driver seat. The aim of testing of the sensors was to see how reconstructed velocity signals should affect the output signals of the developed controllers to the MRA (Sapiński and Rosół, 2004).

2.   Model of a driver seat with controllable damping

The model of a driver seat is shown in Fig. 1. This is a two-degree of freedom (2DOF) system with the following designations: k_1 – stiffness of the suspension system; c_r – damping constant of the suspension system, m_1 – suspension mass (mass of the seat with the cushion); k_2 – stiffness of the cushion; c_2 – damping constant of the cushion; m_2 – body mass (mass of the driver); x_0 – displacement input excitation; x_1 – seat displacement; x_2 – driver displacement.

Let us assume that the seat cushion is removed ($k_2 = 0$, $c_2 = 0$) and denote the total mass of the driver and the seat with no cushion by m. That yields a model of the driver seat with a 1 DOF system. Taking into account that x_{10} is the static position of the seat, l_1 – initial length of the suspension spring, we obtain the following equation of motion for the seat-driver system (dry friction is neglected)

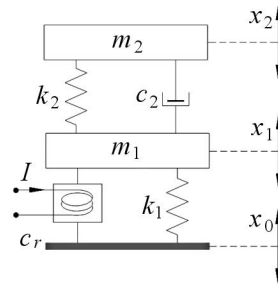$$m_1\ddot{x}_1 + c_r\dot{x}_1 + k_1x_1 = c_r\dot{x}_0 + k_1x_0 \qquad (2.1)$$

Fig. 1. The model of a driver seat

with the initial condition $x_{10} = x_1(t) = l_1 - mg/k_1$, $(g$ – acceleration of gravity).

Equation (2.1) corresponds to the transfer function

$$G(s) = \frac{X_1(s)}{X_0(s)} = \frac{c_r s + k_1}{m_1 s^2 + c_r s + k_1} \tag{2.2}$$

Assuming that $k_1 = 36861\,\text{N/m}$, $m = 112\,\text{kg}$, the undamped natural frequency of the system f_0 is about $2.9\,\text{Hz}$ and the cross-over frequency is $f_c = \sqrt{2}f_0 = 4.1\,\text{Hz}$ (f_c is such a frequency that displacement transmissibility is $X_1(s)/X_2(s) = 1$). In Fig. 2 we show the acceleration transmissibility of a 1 DOF system obtained for the above values of k_1 and m and values of c_r corresponding to the following current levels in the MRA coil (I): $0.00\,\text{A}$, $0.05\,\text{A}$, $0.10\,\text{A}$, $0.15\,\text{A}$. It is readily seen that the resonance frequency of the system with no current is about $3.1\,\text{Hz}$ and it increases with the current level. Simultaneously, it is apparent that rapid damping of free vibrations is provided by the value of current in the range $(0.05, 0.15)\,\text{A}$.
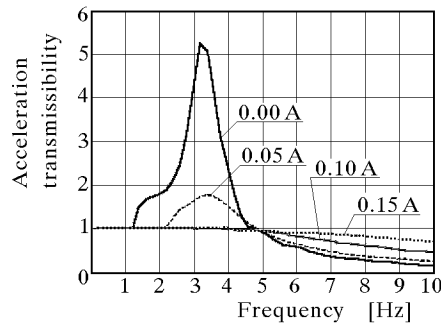

Fig. 2. Acceleration transmissibility for the driver seat

3. Magnetorheological shock absorber

The RD-1005-3 is a small and compact MRA with simple electronics, low voltage and current demands that enables real-time damping adjustment (Fig. 3). This MRA has ±25 mm stroke. The input voltage is 12 V DC and input current can be varied in the range (0,2) A. The response time (dependent on an amplifier and power supply) is less than 25 ms (time to reach 90% of maximun level during a 0 A to 1 A step input at the velocity of 51 mm/s).

Fig. 3. The RD-1005-3 – a general view

The advantage of the MRA is associated with the capability of continuous modification of damping characteristics over the controllable range. This is well seen when we consider the RD-1005-3 family performance curves determined experimentally for the assumed current and velocity ranges (see Fig. 4). These performance curves illustrate a relationship between the force produced by the MRA (output) and shaft velocity (disturbance) that can be adjusted by the magnetic field (control) induced by the applied current.
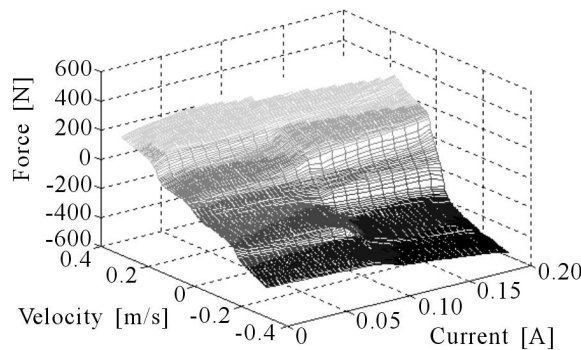

Fig. 4. Performance curves for the RD-1005-3

4. Sensors

A schematic depiction of the driver seat-MRA system in which the control method for a controllable damper patented in (U.S. Patent 5,712, 783, 1998)

can be implemented, reveals that the system requires one accelerometer and one displacement sensor. It was mentioned that the controllers for the MRA made use of velocity signals from the suspension components of the driver seat. That means that the velocity signals have to be reconstructed from output signals of the sensors above. In order to see the reconstructed velocity signals, the investigations for the driver seat-MRA system were realised by experimental testing for available sensors which can be employed in the measurement system of the laboratory setup for the driver seat.

In the tests, we used a linear displacement transmitter of PSz20 series (http://www.peltron.home.pl, 2004) and an accelerometer of ADxL210 series (Analog Devices, 1999). The PSz20 is based on a differential transformer, placed in a cylindrical housing together with an electronic system that can be employed in static and dynamic measurements of the displacements. The ADxL210 is a high-performance 2-axis integrated accelerometer that can measure both dynamic acceleration (e.g., vibration) and static acceleration (e.g., gravity). It produces digital outputs whose duty cycles (ratio of pulse width to period) are proportional to the acceleration in each of the 2 axes. Basic technical specifications for the PSz20 and ADxL210 are provided in Table 1.

Table 1. Technical specifications for the PSz20 and ADxL210

Parameter	Value	
	PSz20	ADxL210
Measurement range	$\pm 10 \cdot 10^{-3}$ m	± 10 g
Power supply	± 15 V DC	$+3, +5.25$ V DC
Output signal	± 5 V DC	PWM (frequency depends on an external resistor)
Pass band	3 dB, 50 Hz	3 dB, 500 Hz (PWM out) 3 dB, 5000 Hz (analog out)
Non-linearity	$\leqslant 0.5\%$	0.2%
Operating temperature	$-20 \ldots + 70°$C	$0 \ldots + 70°$C
Shock survival	100 g, $11 \cdot 10^{-3}$ ms	1000 g

The PSz20 and ADxL210 sensors (see Fig. 5) were tested in the experimental setup shown schematically in Fig. 6. The setup comprises: electro-dynamic shaker, power amplifier (for shaker control), PC with a multi I/O board of RT-DAC4 series (Inteco Ltd., 2002) operating in the system of Windows 2000

through the MATLAB/Simulink (for acquisition and analysis of measurement data).
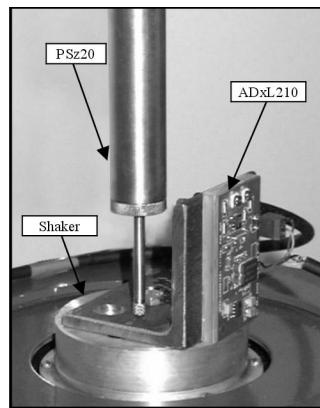

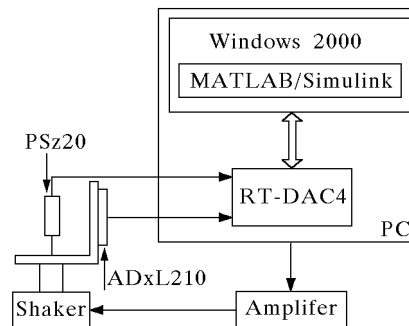Fig. 5. The PSz20 and ADxL210 in the experimental setup – ready for tests

Fig. 6. A diagram of the experimental setup for testing of the PSz20 and ADxL210

The tests were performed for sine excitations with the frequency $(1,10)$ Hz and amplitude $3 \cdot 10^{-3}$ m. Basing on a duly measured output voltage signal of the PSz20, velocity and acceleration signals were reconstructed. Similarly, the velocity and displacement signals were reconstructed from the output voltage signal of the ADxL210. The methods used for the signals reconstruction were discussed in (Sapiński and Rosół, 2004). Some selected results are presented below to see the reconstructed velocity signals.

In Fig. 7 we show velocity signals which were reconstructed from displacement and acceleration signals measured by the PSz20 and ADxL210 at the frequency 5 Hz. It is readily apparent that the reconstruction was quite correct and no phase shifts or transients were observed. The appearing distortions

come as a result of numerical differentiating of the displacement signal, a procedure available in the MATLAB/Simulink. Note that the methods involving the reconstruction of velocity signals from the ADxL210 require a certain time for transient states to stabilize. This time period gets longer with increased excitation frequency. The length of this time period is affected by parameters of a low-pass filter.
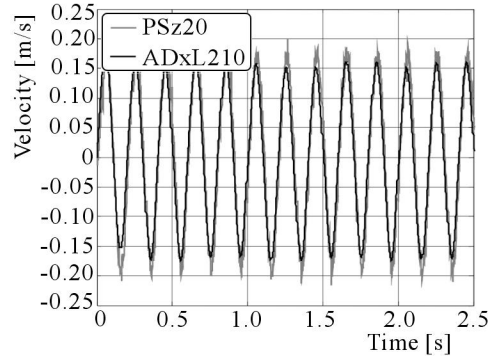

Fig. 7. Reconstructed velocity signals from the PSz20 and ADxL210

When a displacement signal was reconstructed from the ADxL210 output, the integrating circuits cause that the signal stabilization takes longer. That is illustrated for a sine excitation of 5 Hz in Fig. 8. It is worthwhile to mention that the reconstruction of the displacement signal from the ADxL210 output brings about the loss of vital information about the constant component of the displacement.
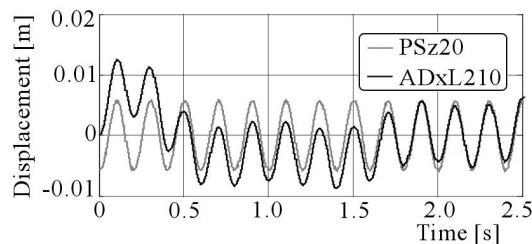

Fig. 8. A reconstructed displacement signal from the ADxL210 compared with the PSz20

When a acceleration signal was reconstructed from the PSz20, major distortions appeared as a result of the use of a double differentiation procedure (available in the MATLAB/Simulink) and a low-pass filter. That is shown for a sine excitation of 5 Hz in Fig. 9. The observed signal distortions might be

reduced by providing low-pass filters or by applying the method of signal sample averaging on the basis of neighbouring samples used in the reconstruction procedure (Sapiński and Rosół, 2004). An increase in the excitation frequency improves the quality of the signal reconstructed from the PSz20.
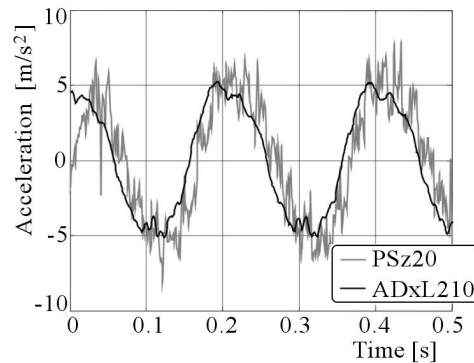

Fig. 9. A reconstructed acceleration signal from the PSz20 compared with the ADxL210

It is reasonable to assume that in the experiments with a driver seat-MRA system with the feedback configuration, two PSz20 sensors would be used. That means that the input signals of the controllers to be developed (e.g. absolute seat velocity and relative velocity – difference between seat velocity and shaker-base velocity) will be reconstructed basing on signal outputs of the PSz20 sensors. In the case of an *on-off* controller, the output signal (the current in the MRA coil) causes the switching between *on* and *off* damping states, depending on the sign of the velocity product (e.g. product of absolute velocity and relative velocity). For the sake of illustration, we compared the signals of reconstructed seat velocity (Fig. 10), velocity product (Fig. 11) and current in the MRA coil (Fig. 12) obtained by the use of PSZ20 and ADxL210 for a sine excitation (frequency $5\,\mathrm{Hz}$, amplitude $1.6 \cdot 10^{-3}\,\mathrm{m}$). Note that the maximum current level at the *on-off* controller output was kept $0.10\,\mathrm{A}$ throughout.

When analysing plots in Fig. 10, it is readily seen that the signal of seat velocity reconstructed from the ADxL210 output stabilized after about $2\,\mathrm{s}$. The transients are responsible for erroneous calculation of the initial velocity product (Fig. 11) and current (Fig. 12a). For time periods in excess of $2\,\mathrm{s}$, currents produced on the basis of reconstructed velocity signals obtained from PSz20 and ADxL210 are similar (Fig. 12b). The differences in reconstructed velocity signal patterns from ADxL210 and PSz20 are attributable to the method of hardware processing of signals from the sensors. These differences become more marked as the frequency increases.
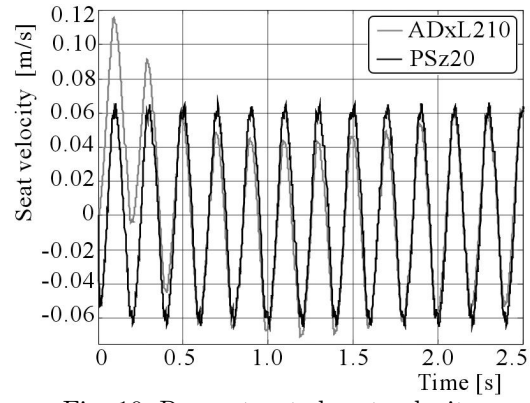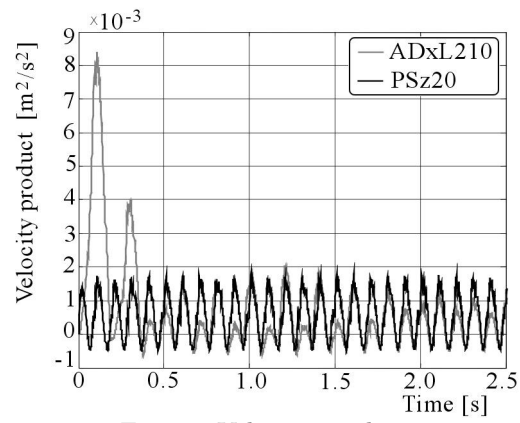
Fig. 10. Reconstructed seat velocity
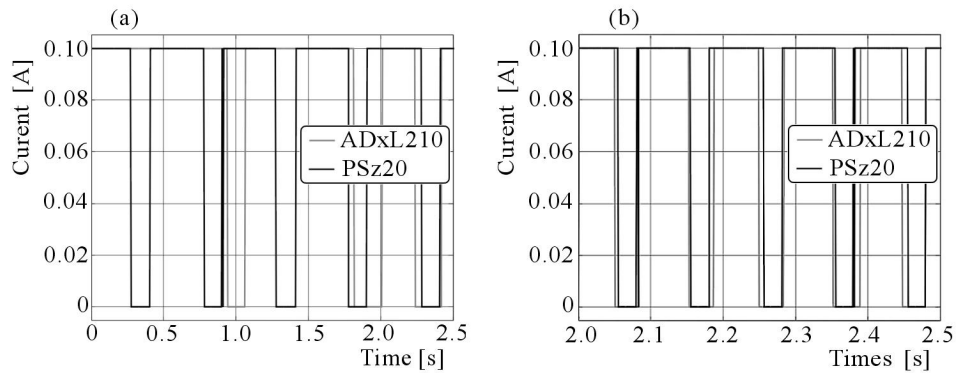

Fig. 11. Velocity product

Fig. 12. Current in the MRA coil: (a) range $(0.0, 0.5)$ s, (b) range $(2.0, 2.5)$ s

Note that at the current stage of experiments, the ADxL210 was used only to compare the signals of measured acceleration with those of acceleration reconstructed from displacements measured by the PSz20 (i.e. it was not employed any more in further experiments conducted for the driver seat-MRA feedback system configuration).

5. Controllers

Among a variety of design approaches to controllers for the MRA in a driver seat support, we present three real-time controllers developed in the integrated environment for design and control of MATLAB/Simulink.

5.1. Control methods

The structure of the developed controllers is shown in Fig. 13. The input signals are the seat velocity $\dot{x}_1$ and relative velocity (difference between seat and shaker base velocities), $(\dot{x}_1 - \dot{x}_0)$, while the output signal is the current in the MRA coil (I).
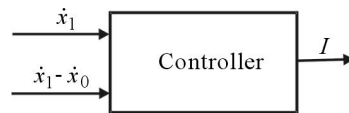

Fig. 13. The structure of controllers

Let us assume that the controllers are denoted by CON1, CON2, CON3 and governed by following formulas

$$\text{CON1:} \quad I = \begin{cases} c_1 & \text{for} \quad \dot{x}_1(\dot{x}_1 - \dot{x}_0) \geqslant 0 \\ 0 & \text{for} \quad \dot{x}_1(\dot{x}_1 - \dot{x}_0) < 0 \end{cases}$$

$$\text{CON2:} \quad I = \begin{cases} c_2|\dot{x}_1 - \dot{x}_0| & \text{for} \quad \dot{x}_1(\dot{x}_1 - \dot{x}_0) \geqslant 0 \\ 0 & \text{for} \quad \dot{x}_1(\dot{x}_1 - \dot{x}_0) < 0 \end{cases} \quad (5.1)$$

$$\text{CON3:} \quad I = \begin{cases} c_3(t)|\dot{x}_1 - \dot{x}_0| & \text{for} \quad \dot{x}_1(\dot{x}_1 - \dot{x}_0) \geqslant 0 \\ 0 & \text{for} \quad \dot{x}_1(\dot{x}_1 - \dot{x}_0) < 0 \end{cases}$$

where

$\dot{x}_0, \dot{x}_1$ — base and seat velocity, respectively
$\dot{x}_1 - \dot{x}_0$ — relative velocity
c_1, c_2 — constants
$c_3(t) = c_3^*(t) = G_3|\dot{x}_1|$ — continuously variable factor
$G3$ — gain factor.

Note that the values of c_1, c_2 and G_3 depend on the maximum level of current applied to the MRA coil.

It is readily seen that CON1 is an *on-off* controller (i.e. it involves the switching between the minimum and maximum damping levels) while CON2 and CON3 are continuous controllers (i.e. the number of damping levels is greater, as continuously variable damping coefficients may be obtained).

5.2.   Integrated environment for design and control

Real-time controllers for the MRA were implemented in the integrated design and control environment including the following hardware and software:

- PC (Pentium III/1GHz) with a multi I/O board of RT-DAC4 series

- operating system MS Windows 2000

- MATLAB/Simulink (version 6.5)

- Real Time Workshop (RTW) toolbox in MATLAB/Simulink with the extension Real Time Windows Target (RTWT).

The MATLAB/Simulink was used to support design of the controllers. The toolbox RTW extends potential applications of the MATLAB/Simulink to control by providing the path of "rapid prototyping" (Grega, 1999). That allows real time implementation of control algorithms directly from Simulink. Unfortunately, the toolbox RTW is not capable of generating real-time tasks in the MS Windows environment, that is why the integrated design and control environment is supported by the RTWT software. Communication procedures featured by RTWT allow compilation of an RTW code and admit its real-time operation in MS Windows on a specified hardware platform.

5.3.   Automatic code generation

A block diagram of subsequent stages of *executive file* development using RTWT is shown in Fig. 14. It is based on the Simulink model of the controller. Block designations are provided below.

The block *model.m* includes the Simulink model of the controller. It contains input drivers (being the source of input data for the controller) and output drivers providing for actuators control. The Simulink model of a controller
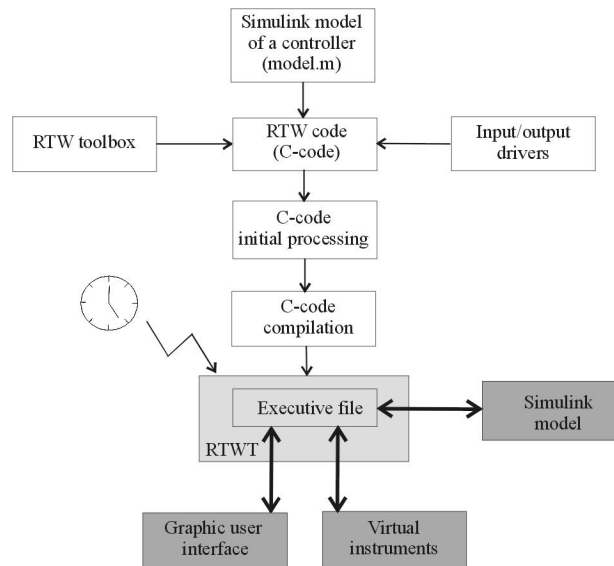
Fig. 14. Use of the RTW toolbox for controller prototyping in MS-Windows

was used to automatically generate a *C-code*, which was then preprocessed and compiled. At the stage of code compilation, an *executive file* was generated. The file is called up and started as a result of clock interrupts operated by the real-time system kernel. An executive file might be connected with the Simulink environment as long as it is started in the external mode (The Math Works, 2003). It might be also connected to virtual elements which enable the tuning of task parameters and signal acquisition and monitoring.

Note that the blocks in the diagram coloured bright grey represent real-time tasks, while those coloured dark grey – *on-line* tasks. The black thick lines connecting the blocks illustrate the flow of information and command signals within the system.

A model of a Simulink controller is shown in Fig. 15. It is controller CON1, implementing *on-off* control in accordance with formula $(5.1)_1$. Integrated Simulink blocks are used as controller blocks. Measurement data (shaker base displacements and seat displacements) from the input driver (block *RT-DAC4 Analog inputs*) supporting A/C converters on the board RT-DAC4 are transformed to the shape required by the controller algorithm. The control signal for the MRA is sent to the output drivers (block *RT-DAC4 PWM0*), following conversion of the signal from the controller (block *I/PWM*) and taking into account the constraints upon the maximal current in the MRA coil (block *Saturation 1*). Besides, the parameters of signals applied to the shaker can

be controlled too, using the output driver (block *RT-DAC4 Analog outputs*) controlling the C/A converters in the RT-DAC4 board. The maximal signal constraint is taken into account in block *Saturation 2*. Block *Scope* is used for data acquisition and monitoring.
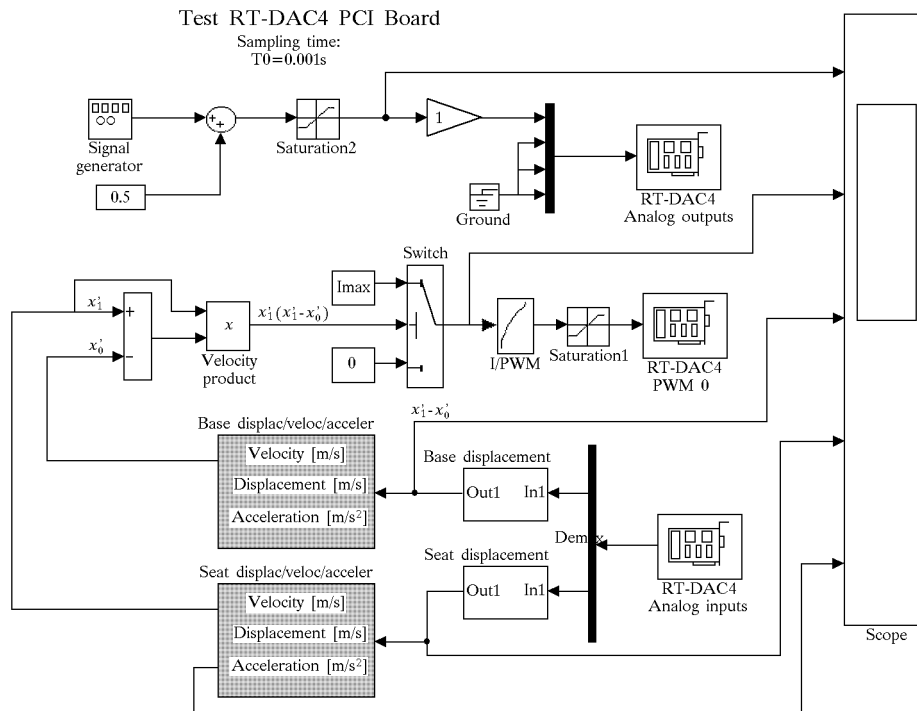

Fig. 15. Controller CON1 ready for interaction with the RTW toolbox

6.   Experiments

The driver seat-MRA system was experimentally tested in open loop and feedback system configurations under harmonic and shock excitations.

6.1.   Experimental setup

A diagram of the experimental setup used for testing of real-time controllers is depicted in Fig. 16. The electro-hydraulic shaker was supplied via a hydraulic pump and controlled from a control cubicle. Input-output data were acquired using a data acquisition and control system based on a PC (Pentium III/1

GHz) with the multi PCI I/O board of RT-DAC4 series operating in the software environment of Windows 2000, MATLAB/Simulink and RTW with RTWT. The seat with no cushion (equipped with the MRA of RD-1005-3 series and a designed spring) to be tested is shown in Fig. 17.
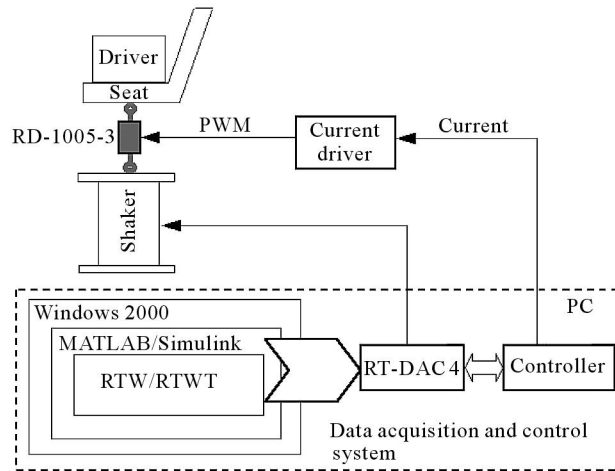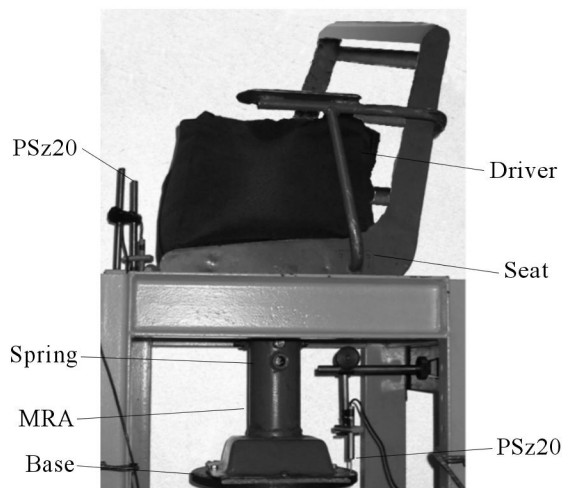
Fig. 16. A diagram of the experimental setup

Fig. 17. The driver seat in the experimental setup

The total mass of the driver and seat with no cushion was 112 kg and the spring constant was 36861 N/m. Displacements of the shaker-base and driver seat were measured by two PSz20 sensors. The input signals for the controllers

were the seat velocity and relative velocity, while the output signal was the current in the MRA coil.

6.2. Performance testing for vibration isolation

At the first stage, the open loop system was investigated. Driver seat responses were measured under sine excitations of the shaker base with the amplitude $1.5 \cdot 10^{-3}$ m in the frequency range $(1,10)$ Hz for the following current levels in the MRA coil: 0.00 A, 0.05 A, 0.10 A, 0.15 A. The obtained results are shown in Fig. 18 in the form of acceleration transmissibility.
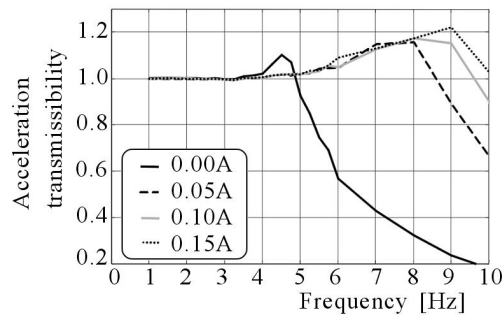
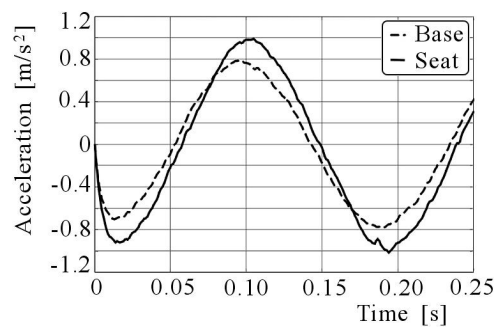Fig. 18. Acceleration transmissibility in the open loop system

Fig. 19. Seat acceleration in the open loop system

Figure 18 shows that as the level of current increases, the resonance frequency of the system will increase too, and the frequency at which vibration control of the seat is most effective ranges from 3 Hz to 5 Hz. Fig. 19 shows time variations of the seat acceleration in response to the sine excitation with the frequency 5 Hz (e.g. near-resonance frequency of the investigated system). Note that the current was set as 0.00 A. It is clearly seen that the system enhanced the input signal and shifted the phase.

At the second stage, feedback system configurations with CON1, CON2 and CON3 were tested under the same sine excitations as for the open loop system. The sampling rate for real time tasks was 0.001 s. The constants assumed in control schemes were as follows: for CON1 – $c_1 = 0.10$, CON2 – $c_2 = 60$, CON3 – $G = 9000$. These values would yield the maximum current level which was assumed to be 0.10 A. Selected results of the experiments are presented in the frequency and time domain (see Fig. 20 and Fig. 21).
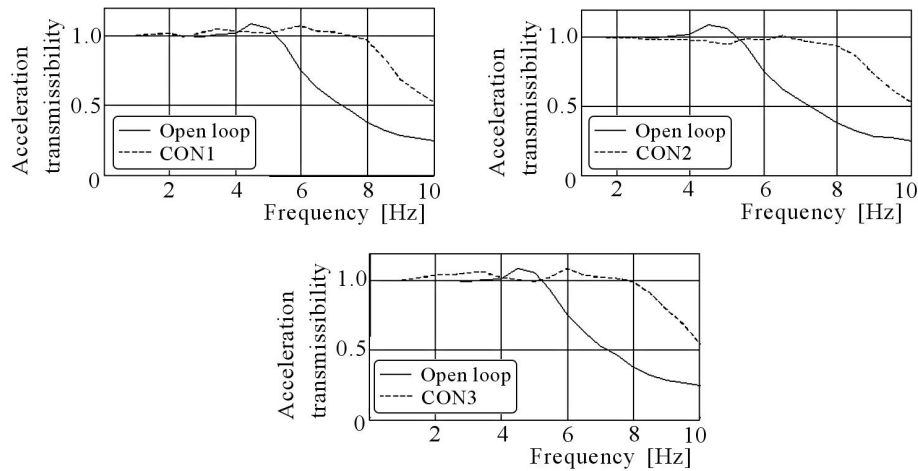

Fig. 20. Acceleration transmissibility in the open loop and feedback system configurations

In Fig. 20, the acceleration transmissibility for each feedback system configuration is plotted and comparison is made to the open loop system. A close survey of the plots reveals that the best performance was achieved in the feedback system with CON2 (Sapiński, 2004).

Figure 21 shows time patterns of the current, velocity product and seat velocity for feedback system configurations with CON1, CON2 and CON3 at the frequency 5 Hz. These results confirm the operating principle of the developed controllers. In the case of CON1, the current was switched between two values, i.e. 0.00 A and 0.10 A, while in the case of CON2 and CON3 the current may assume any value from the range (0.00,0.10) A.

Note that an undesirable phenomenon was observed in all tested feedback system configurations. It is known as the chattering effect (current was produced in states when the velocity product oscillated around zero value), however it seems to be predominant in the feedback system with CON1.
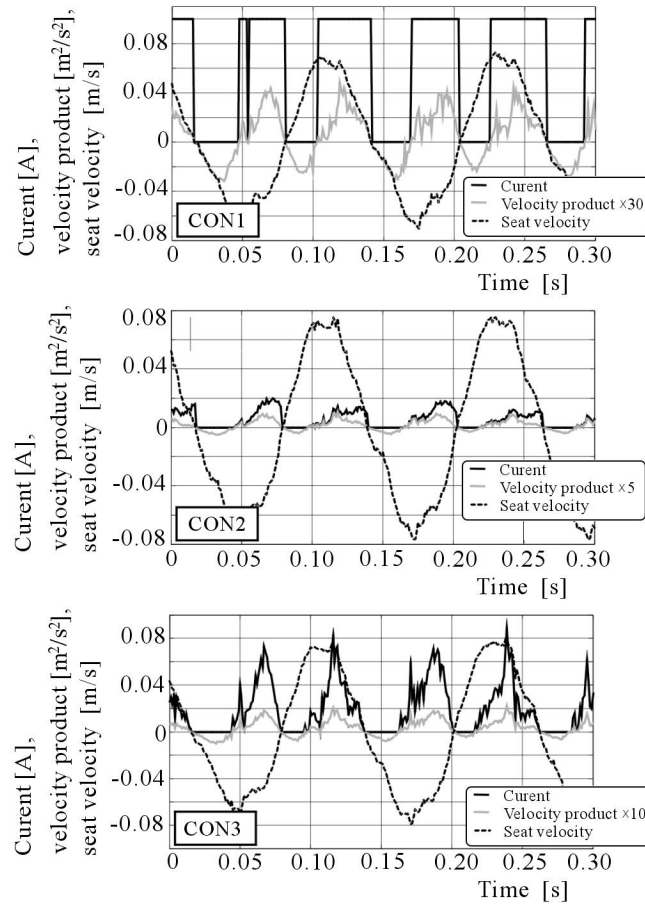
Fig. 21. Current, velocity product, seat velocity in feedback system configurations

To illustrate the effectiveness of CON1, CON2 and CON3, we show zoomed sections of time patterns for driver seat acceleration in open loop and feedback system configurations (see Fig. 22).

6.3. Performance testing for shock isolation

At this point, we present results of tests on the driver seat-MRA system under rounded pulse shocks. The rounded pulse shock is analytically expressed by the formula

$$x_0(t) = X_0 \frac{\mathrm{e}^2}{4} \gamma \omega_n t \mathrm{e}^{-\gamma \omega_n t} \tag{6.1}$$

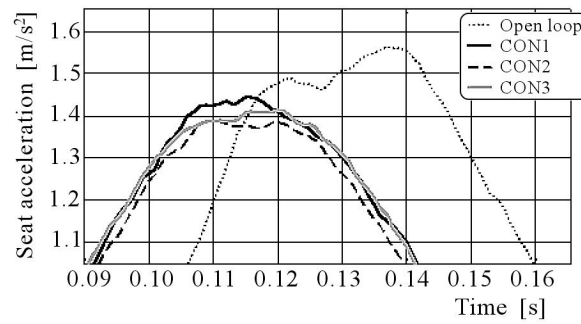where γ is a parameter expressing time of pulse duration in relation to the

Fig. 22. Zoomed sections of seat acceleration in open loop and feedback system configurations

half-period of natural system vibrations. The parameter γ is given by the formula

$$\gamma = \frac{T}{2\tau} = \frac{\pi}{\omega_n \tau} \tag{6.2}$$

where

τ – duration of a square impulse with the area equal to that of the rounded pulse

ω_n – pulsation of natural vibrations of the system

X_0 – rounded pulse amplitude.

The chief advantage of the rounded pulse excitation is that its first and second derivative assume limited values for all time instants t. The desired amplitude of a rounded pulse was set to be $X_0 = 2.57 \cdot 10^{-3}$ m (Liu *et al.*, 2002). After rescaling associated with signal passing through a C/A converter of RT-DAC4 and amplifiers of the control cubicle of the shaker, the maximum value of the rounded pulse was $1.75 \cdot 10^{-3}$ m. In Fig. 23 plots of pulses applied in experiments for various values of γ are shown.

Results of experiments conducted in the open loop system configuration for the rounded pulse excitation applied to the shaker-base are depicted in Fig. 24 and Fig. 25.

It appears that when the value of γ was lower (e.g. time of rounded pulse duration got longer), the maximum value of driver seat acceleration was greater (see Fig. 24). Moreover, time required for the system to reach the steady state got shorter. Similarly, when analyzing plots in Fig. 25, we see that as the current level increased, the maximal value of driver seat acceleration decreased. Throughout the investigated range of the current there were no changes in the time required to reach the steady state.
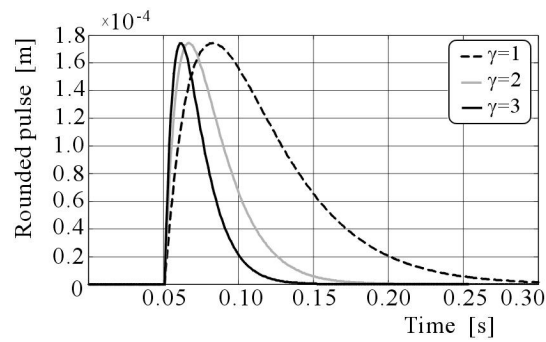
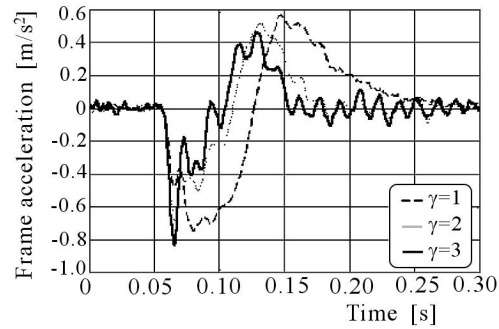Fig. 23. Rounded pulse excitation for various values of γ

Fig. 24. Seat acceleration in response to the rounded pulse for various values of γ
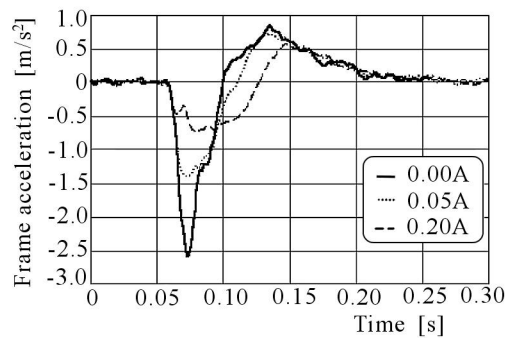and the current $0.00\,\text{A}$

Fig. 25. Seat acceleration in response to the rounded pulse for various current levels
at $\gamma = 1$

Selected results of experiments conducted in feedback system configurations with CON1 and CON2, and compared with those achieved in the open loop system are shown for two different values of γ in Fig. 26.
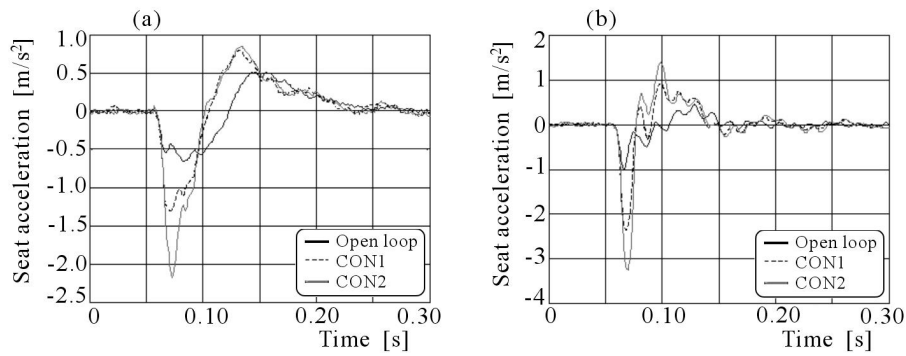
Fig. 26. Seat acceleration in response to the rounded pulse for: (a) $\gamma = 1$, (b) $\gamma = 3$

It is readily apparent that those feedback systems did not provide any reduction to the seat acceleration when compared to the open loop system, and neither did the system equipped with CON3. That may be explained by the fact that the system response to current changes was prolonged. The reasons for such a state of affairs might be as follows: nonzero time of MRA force stabilisation, magnetic residues in MRA components, delays due to current stabilisation at the output of the current driver.

7. Conclusions

The paper is concerned with an experimental study of real-time control of an MRA employed in a driver seat suspension. The driver seat-MRA system was tested in open loop and feedback configurations for vibration and shock isolation. The designed real-time controllers (CON1, CON2, CON3) for the MRA implement *on-off* and continuously variable control schemes utilising velocity signals from the driver-seat components. For this reason, special attention was given to sensors used in the experiments which were tested to see how reconstructed velocity signals should affect output signals of the controllers to the MRA. Controllers CON1, CON2, CON3 were developed in the integrated design and control environment of the MATLAB/Simulink. The performance of the driver seat-MRA system in open loop and feedback configurations was investigated under harmonic and shock excitations. The analysis of the performance factors for vibration isolation revealed that CON2 had the best features. Tests revealed also the presence of undesirable phenomena during operation of the controllers (e.g. chattering effect). That applies to all con-

trollers, however it seems to be predominant in controller CON1. Similar tests for the driver seat-MRA system were conducted under shock (rounded-pulse) excitations. The comparison of system responses in open loop and feedback configurations (with controllers CON1 and CON2) lead us to the conclusion that the action of the developed controllers fails to reduce the acceleration in the system. The reasons for this state of affairs are attributable to the properties and operating principles of the electromagnetic circuit of the MRA employed in the investigated driver seat.

Research is now underway to develop real-time controllers for MRAs in driver seat supports on digital microcontrollers.

References

1. AHMADIAN M., 1999, On the isolation properties of semi-active dampers, *Journal of Vibration and Control*, 217-232

2. GREGA W., 1999, *Sterowanie cyfrowe w czasie rzeczywistym*, Krakw

3. LIU Y., MACE B., WATERS T., 2002, Semi-active dampers for shock and vibration isolation: algorithms and performance, *Proc. of the Int. Symp. on Active Control of Sound and Vibration*, UK, 1121-1132

4. SAPIŃSKI B., 2004, Linear magnetorheological fluid dampers for vibration mitigation: modelling, control and experimental testing, *Rozprawy Monografie AGH*, **128**

5. SAPIŃSKI B., 2005, Fuzzy control for MR damper in a driver's seat, *Journal of Theoretical and Applied Mechanics*, **43**, 1, 179-201

6. SAPIŃSKI B., ROSÓŁ M., 2004, Processing of measurement signals for MR damper control in suspension systems, *Proc. of the Int. Symp. on Active Control of Sound and Vibration*, USA, 1-9

7. ANALOG DEVICES, 1999, ADxL202/210. Low Cost $\pm 2/\pm 10$ g Dual Axis Accelerometer with Digital Output, Data Sheet, USA

8. INTECO LTD., 2002, User's guide, RT-DAC4 multi I/O board

9. LORD CORPORATION, 2003, http://www.lord.com

10. MOTION MASTER SYTEM, 2004, http://www.lord.com

11. PELTRON LTD., 2004, *Transformer linear displacement transmitters PSz series*, http://www.peltron.home.pl

12. THE MATH WORKS INC., 2003, *Real Time Workshop User's Guide*

13. U.S. PATENT No. 5,652,704, 1997, *Controllable Seat Damper and Control Method Therefore*

Sterowanie w czasie rzeczywistym amortyzatora magnetoreologicznego w fotelu kierowcy

Streszczenie

Artykuł podsumowuje badania autora dotyczące sterowania w czasie amortyzatora magnetoreologicznego (MR) w fotelu kierowcy. Wykonano eksperymenty, których celem było zbadanie skuteczności amortyzatora do tłumienia drgań i wstrząsów w otwartym i zamkniętym układzie sterowania. Regulatory czasu rzeczywistego typu dwupołożeniowego i ciągłego dla amortyzatora zrealizowano w zintegrowanym środowisku projektowania i sterowania MATLAB/Simulink. Przeprowadzono testy, obrazujące wpływ odtworzonych na podstawie sygnałów uzyskanych z czujników przemieszczenia i przyspieszenia sygnałów prędkości na sygnały wyjściowe regulatorów.